THE ASTRONOMICAL JOURNAL, 120:189–202, 2000 July

SPECTROSCOPIC OBSERVATIONS OF MERGING GALAXIES[1]

C. J. DONZELLI[2]
IATE, Observatorio Astronómico, Universidad Nacional de Córdoba, Laprida 854, 5000, Córdoba, Argentina
AND
M. G. PASTORIZA[2]
Departamento de Astronomia, IF-UFRGS, C.P. 15051, CEP 91501-970, Porto Alegre, RS, Brazil
Received 2000 February 3; accepted 2000 April 6

ABSTRACT

In this paper we describe the spectroscopic and infrared properties of a sample of 25 merging galaxy pairs, selected from the catalog of Arp & Madore, and we compare them with those observed in a similar sample of interacting galaxies (Donzelli & Pastoriza). It is noted that mergers as well as interacting systems comprise a wide range of spectral types, going from those corresponding to well-evolved stellar populations (older than 200 Myr) to those that show clear signatures of H II regions with stellar populations younger than 8 Myr. However, merger galaxies show on average more excited spectra than interacting pairs, which could be attributed to lower gas metallicity. From the emission lines we also found that merging systems show on average higher (about a factor of 2) star formation rates than interacting galaxies. Classical diagnostic diagrams show that only three of 50 of the galaxies (6%) present some form of nuclear activity: two Seyfert galaxies and one LINER. However, through a detailed analysis of the pure emission-line spectra, we conclude that this fraction may raise up to 23% of the mergers if we consider that some galaxies host a low-luminosity active nucleus surrounded by strong star-forming regions. This latter assumption is also supported by the infrared colors of the galaxies. Regarding to the total infrared luminosities, the merging galaxies show on average an IR luminosity, $\log (L_{\rm ir}) = 10.7$, lower than that of interacting systems, $\log (L_{\rm ir}) = 10.9$. We find that only three mergers of the sample (12%) can be classified as luminous infrared galaxies, while this fraction increases to 24% in the interacting sample.

Key words: galaxies: interactions — galaxies: nuclei — galaxies: Seyfert

1. INTRODUCTION

The steadily growing theoretical and observational data indicate that galaxy interactions can deeply affect their evolution and stellar populations. In general terms we know so far that interacting galaxies are more active in the UV (Larson & Tinsley 1978), in the near-infrared (Joseph & Wright 1985), in optical emission-line strength (Kennicutt & Keel 1984), and in radio emission (Stocke 1978; Hummel 1981).

It is also widely admitted that ultraluminous infrared galaxies, a class of objects with luminosity above $10^{12}\ L_{\odot}$, are interacting or merging systems (Sanders et al. 1988; Melnick & Mirabel 1990). The power source of their enhanced infrared luminosity is probably due to the presence of starburst or AGN activity or a combination of both, but its true nature still remains unanswered (Duc, Mirabel, & Maza 1997).

We have begun a series of photometric and spectroscopic observations of two samples of interacting and merging galaxies in order to address some questions related to nuclear activity, star formation, and stellar populations.

In a first paper Donzelli & Pastoriza (1997, hereafter DP97) presented spectroscopic observations of 49 galaxy pairs and concluded that, despite the very large range of spectral properties present in the interacting pairs, the star formation is enhanced nearly a factor of 2 when compared with isolated galaxies. Moreover, this enhancement of star formation activity is much more pronounced (50%) in the minor component of the pairs. On the other hand, no Seyfert-type nuclei were found in the sample. As an explanation, based on the spectral characteristics of the sampled galaxies, we propose that the lack of AGNs is due to the dilution of the AGN spectra by circumnuclear star-forming regions (Pastoriza, Donzelli, & Bonatto 1999, hereafter PDB99). As a result, nearly 40% of the interacting pairs may host a low-luminosity AGN. This fraction is consistent with the previous results published by Ho, Filippenko, & Sargent (1997), who found in a nearly complete magnitude-limited sample of emission-line galaxies that around 50% of the objects have some form of AGN, or composite LINER/H II spectrum.

Our goal in this paper is to determine the spectroscopic and infrared properties of a sample of merging galaxies, selected from the catalog of Arp & Madore (1987, hereafter AMC) and to compare them to those observed in the galaxy pairs described in DP97.

The paper is structured as follows: in § 2 we describe the sample selection; in § 3 we give the observations and data reduction; and in § 4 we analyze the spectroscopic results, the star formation rates and diagnostic diagrams. Section 5 describes the infrared luminosities. Conclusions are summarized in § 6.

2. SAMPLE SELECTION

For this work we optically selected a sample of merging galaxies from the AMC following these main critera established by Heckman (1983): Both galaxies of the system (1)

[1] Based on observations made at CASLEO. Complejo Astronómico El Leoncito is operated under agreement between the Consejo Nacional de Investigaciones Científicas y Técnicas de la República Argentina and the National Universities of La Plata, Córdoba and San Juan.
[2] Visiting Astronomer at CASLEO Observatory.

TABLE 1

OBSERVED MERGERS[a]

Name	R.A. (J2000)	Decl. (J2000)	m_b	cz (km s^{-1})	A_v	Locus
AM 0036−432.....	00 39 05	−43 04 49	16.76	3431	0.02	S
AM 0049−412.....	00 52 20	−41 03 45	15.64	...	0.02	W
AM 0112−554.....	01 14 23	−55 23 55	...	3645	0.00	E
AM 0144−330.....	01 46 12	−32 45 49	16.72	...	0.02	S
AM 0223−403.....	02 25 14	−40 25 37	...	11820	0.00	N
AM 0313−545.....	03 15 05	−54 49 12	14.53	8234	0.00	N
AM 0427−545.....	04 29 41	−27 24 31	...	906	0.06	E
AM 0500−620.....	05 00 34	−62 04 06	...	8240	0.00	S
AM 0545−453.....	05 47 15	−45 29 13	14.90	12441	0.13	N
AM 0558−335.....	06 00 04	−33 55 12	14.16	2866	0.05	E
AM 0623−605.....	06 23 46	−60 58 36	15.16	12096	0.10	N
AM 0646−645.....	06 46 51	−64 57 35	...	9056	0.16	S
AM 1018−283.....	10 20 22	−28 52 11	...	...	0.16	E
AM 1054−325.....	10 56 59	−33 09 39	...	...	0.22	S
AM 1204−292.....	12 06 41	−29 45 42	11.60	1936	0.18	W
AM 1204−314.....	12 06 52	−31 56 47	16.00	6845	0.21	S
AM 1316−241.....	13 19 32	−24 29 02	15.71	9554	0.40	N
AM 1325−292.....	13 27 54	−29 37 03	12.83	4281	0.16	E
AM 2039−241.....	20 42 29	−24 09 06	14.66	5860	0.16	S
AM 2143−464.....	21 46 16	−46 30 55	13.64	9666	0.00	N
AM 2225−250.....	22 28 38	−24 50 27	12.81	4347	0.00	E
AM 2244−651.....	22 47 20	−65 03 28	...	3148	0.00	E
AM 2252−340.....	22 52 34	−33 53 29	...	8624	0.00	W
AM 2350−410.....	23 53 19	−40 48 24	14.98	8926	0.00	E
AM 2353−291.....	23 56 24	−29 01 22	...	...	0.00	E

[a] Data are referred to the brighter component.

exhibit morphological perturbation and (2) show superposition of all or part of the galaxy bodies.

The sample was also chosen without regard to the morphological type of the galaxies participating in the merger. Therefore, mergers of both elliptical and spiral galaxies were included.

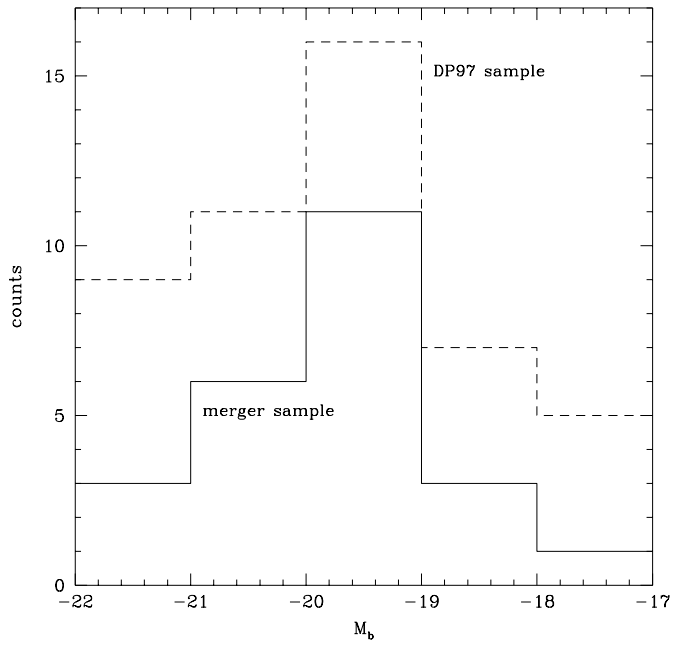

FIG. 1.—Luminosity distribution for the merger sample (*solid line*) and the interacting sample (DP97) (*dashed line*).

A total of 25 systems satisfying the above requirements were observed. These galaxies are listed in Table 1, which specifies the AMC name, right ascension, declination, apparent B magnitude, radial velocity of the brighter component of the merger and blue extinction as listed in the Third Reference Catalogue of Bright Galaxies (de Vaucouleurs et al. 1991, hereafter RC3). The last column specifies the locus (direction on the sky) of the main component.

In order to compare the spectroscopic properties of this sample with those derived from the interacting pairs of DP97, we verified if both components of the merger systems have similar luminosity distribution to that of the pairs. To this purpose we have derived M_b from the apparent integrated magnitudes taken from our data and the RC3 and ESO catalogs. Distances were calculated from the radial velocities derived from our spectroscopic observations. Throughout this paper we have assumed $H_0 = 75$ km s^{-1} Mpc^{-1}. The luminosity distributions for both merger and interacting samples are presented in Figure 1.

3. OBSERVATIONS AND DATA REDUCTION

3.1. *Spectroscopy*

We carried out long-slit spectroscopy using the REOSC Spectrograph at CASLEO 2.15 m Ritchey-Chretien telescope, San Juan, Argentina. The spectrograph has attached a Tektronix 1024^2 CCD with 24 μm pixels. A 300 line mm^{-1} grating giving a resolution of 3.3 Å was used. The galaxies were observed using a slit 2.5 long and 3″ wide in the spectral range 3700–7000 Å. In all cases the slit was oriented so as to include both nuclei involved in the merger.

Spectra were calibrated in wavelength using comparison lines from a He-Ne-Ar lamp. Calibration accuracy was esti-

TABLE 2

SPECTROSCOPIC OBSERVATIONS

Galaxy	Date	Exposure (s)
AM 0036−432.....	1997 Dec 4	3 × 1200
AM 0049−412.....	1997 Dec 3	3 × 1200
AM 0112−554.....	1997 Oct 2	2 × 1800
AM 0144−330.....	1997 Dec 3	3 × 1200
AM 0223−403.....	1997 Dec 4	3 × 1200
AM 0313−545.....	1997 Oct 2	2 × 1800
AM 0427−545.....	1997 Dec 2	3 × 1200
AM 0500−620.....	1997 Dec 4	3 × 1200
AM 0545−453.....	1997 Oct 3	2 × 1800
AM 0558−335.....	1997 Dec 3	3 × 1200
AM 0623−605.....	1998 Feb 28	3 × 900
AM 0646−645.....	1997 Dec 4	3 × 1200
AM 1018−283.....	1998 Feb 28	3 × 900
AM 1054−325.....	1998 Feb 27	3 × 900
AM 1204−292.....	1998 Feb 27	3 × 900
AM 1204−314.....	1998 Feb 28	3 × 900
AM 1316−241.....	1998 Feb 28	3 × 900
AM 1325−292.....	1998 Feb 27	3 × 900
AM 2039−241.....	1997 Oct 2	2 × 1800
AM 2143−464.....	1977 Oct 3	2 × 1800
AM 2225−250.....	1997 Oct 3	2 × 1800
AM 2244−651.....	1997 Oct 2	2 × 1800
AM 2252−340.....	1997 Oct 3	2 × 1800
AM 2350−410.....	1997 Oct 2	2 × 1800
AM 2353−291.....	1997 Oct 3	2 × 1800

mated to be less than 15 km s^{-1}. At least four standard stars were observed each night to flux-calibrate the spectra. These stars were selected from the Catalogue of Southern Spectrophotometric Standards (Stone & Baldwin 1983). Analysis of the system sensitivity function fitting shows that relative fluxes are good to ∼15%. The main error sources were inaccuracies in the continuum subtraction and deblending techniques. Standard data reduction techniques were used to process the data, mainly CCDRED and LONGSLIT packages included in IRAF (developed by NOAO). All spectra were corrected for Galactic absorption using A_v values taken from the RC3. No correction for internal reddening was carried out. Table 2 lists the observation date and exposure for each merger.

4. SPECTROSCOPIC RESULTS

4.1. *Radial Velocities and Equivalent Widths*

Each pair of nuclear spectra was extracted from a rectangular aperture centered at the peaks of the brightness profile. We adopted the name component A for the galaxy with the brighter peak profile at 6400 Å. The spectra of all galaxies in the sample are presented in Figures 2 and 3, in which component A is displayed in the left-hand panel while component B is displayed in the right-hand panel. These figures also specify the corresponding scale of the extracted spectra. Wavelength is expressed in angstroms, and flux is in units of 10^{-15} ergs cm^{-2} s^{-1} $Å^{-1}$.

All spectra are redshift-corrected and are plotted on a common wavelength scale of 3600–7200 Å. Radial velocities were measured from emission and absorption lines using the cross-correlation technique developed by Tonry & Davis (1979) as implemented in the RV task of IRAF. The values obtained are listed in columns (4) and (7) of Table 3. Typical errors are around 75 km s^{-1}.

As in DP97, we have considered as physical pairs those systems with radial velocity differences of less than 400 km s^{-1}. According to this criteria, two systems are apparent mergers; these are AM 1316−241 and AM 2252−340. The spectra of these galaxies are plotted in Figure 3.

Line fluxes were measured on the pure emission-line spectra as described in PDB99. Basically the method is as follows: after correcting for reddening and radial velocity, a suitable stellar population template (Bica 1988) was subtracted from each spectrum in order to eliminate the contribution of the host galaxy to the observed continuum. The resulting fluxes were then corrected for internal extinction assuming an intrinsic Hα/Hβ ratio of 2.85 for those galaxies with H II region–type spectrum and 3.10 for those objects with AGN-type spectrum (Osterbrock 1989). The corresponding emission lines ratios are listed in Tables 4A and 4B for the A and B components, respectively.

4.2. *Spectroscopic Classification*

As in DP97 we classified the merger galaxies in four groups taking into account the emission-line–type spectrum inferred from the [N II] λλ6548, 6584/Hα ratio and the EW(Hα + [N II]) observed in both components. The classification is at follows:

Group 1.—The spectra of both components are dominated by strong absorption features of TiO λ6156, Na λ5890, Mg I + Mg H λ5175, the G band of CH λ4301, CN λ4200, and Ca II λ3933. The galaxies in this group are AM 1204−292, AM 1325−292, AM 2039−241, AM 2225−250, AM 2244−651, and AM 2353−291. A very weak emission line is observed in the A component of AM 2039−241 and in the B component of AM 2225−250 and AM 2353−291. The EW(Hα + [N II]) values for these objects are lower than 5 Å.

Group 2.—In this group we include those mergers for which one component shows the same absorption features as in group 1 while the other component shows an emission-line spectra. This group is formed by AM 0223−403, AM 0500−620, AM 0623−605, and AM 1018−283.

Group 3.—In this group both components show bright emission-line spectra. For at least one of the components, the emission-line intensity ratio [N II]/Hα is equal to or larger than 1; this is characteristic of AGN galaxies. We have included in this group AM 0112−554, AM 0545−453, AM 0646−645, AM 1204−314, AM 2143−464, and AM 2350−410.

Group 4.—Both components clearly show signatures of H II region emission-line spectra similar to that observed in starburst galaxies. A wide range of excitation is observed as can be inferred from the EW(Hα + [N II]) values, which range from 15 to 333 Å. The galaxies in this group are AM 0036−432, AM 0049−412, AM 0144−330, AM 0313−545, AM 0427−273, AM 0558−335, and AM 1054−325. Having this classification in mind we wanted to inspect the morphological types involved in each of these groups. This can be done since we have CCD images for almost the total of the whole sample. For the rest of the galaxies the distinction was made from ESO-SRC survey images. In the first case we classified the galaxies through their luminosity profiles. In the second case the classification was made only by visual inspection, since disk galaxies produce long narrow tail features, while ellipticals

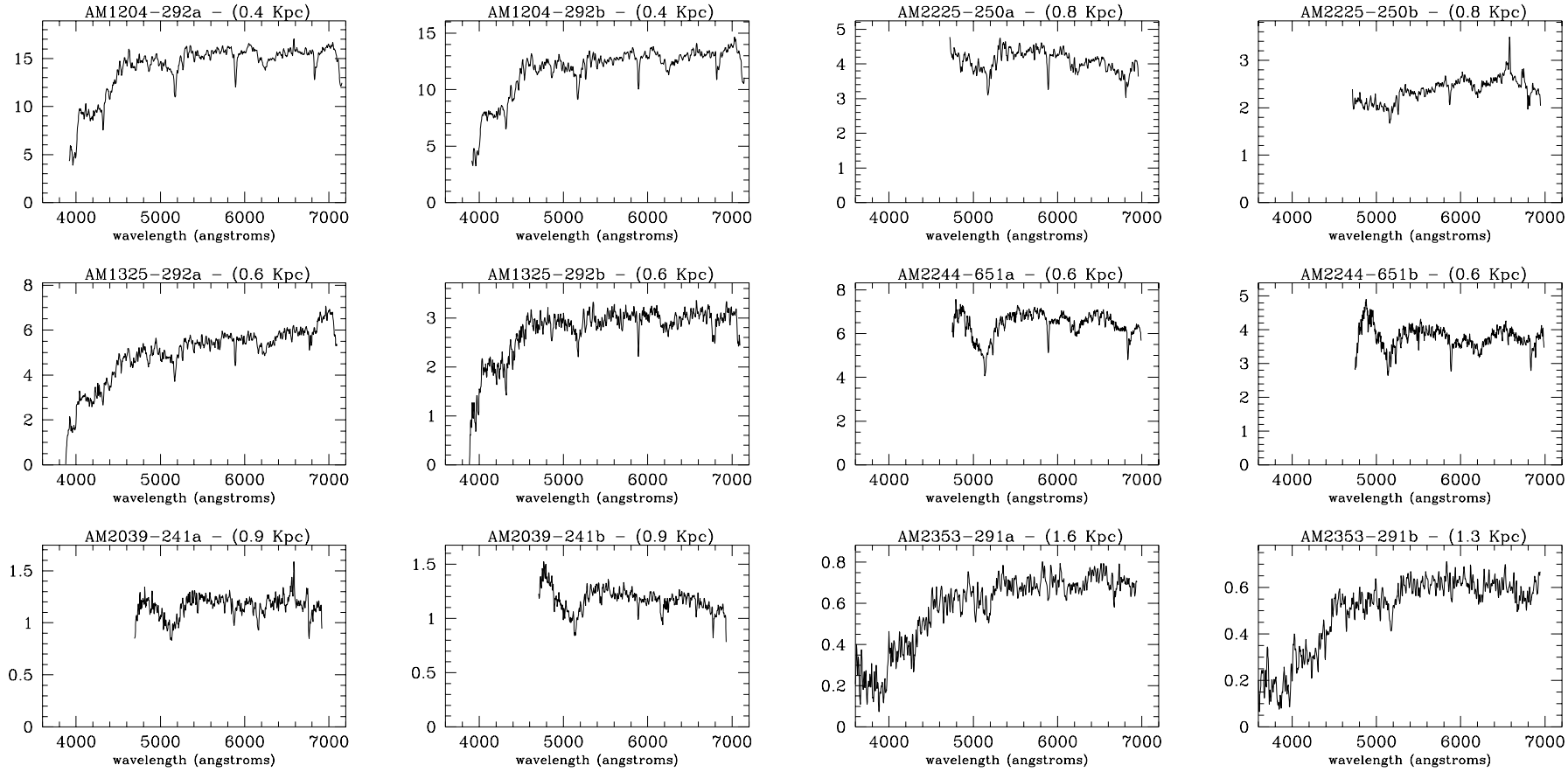

FIG. 2.—Spectra for merger pairs. Component A is displayed in the left-hand panel, and component B is displayed in the right-hand panel. The corresponding scale of the extracted spectra is also specified. Flux is in units of 10^{-15} ergs cm^{-2} s^{-1} Å^{-1}.

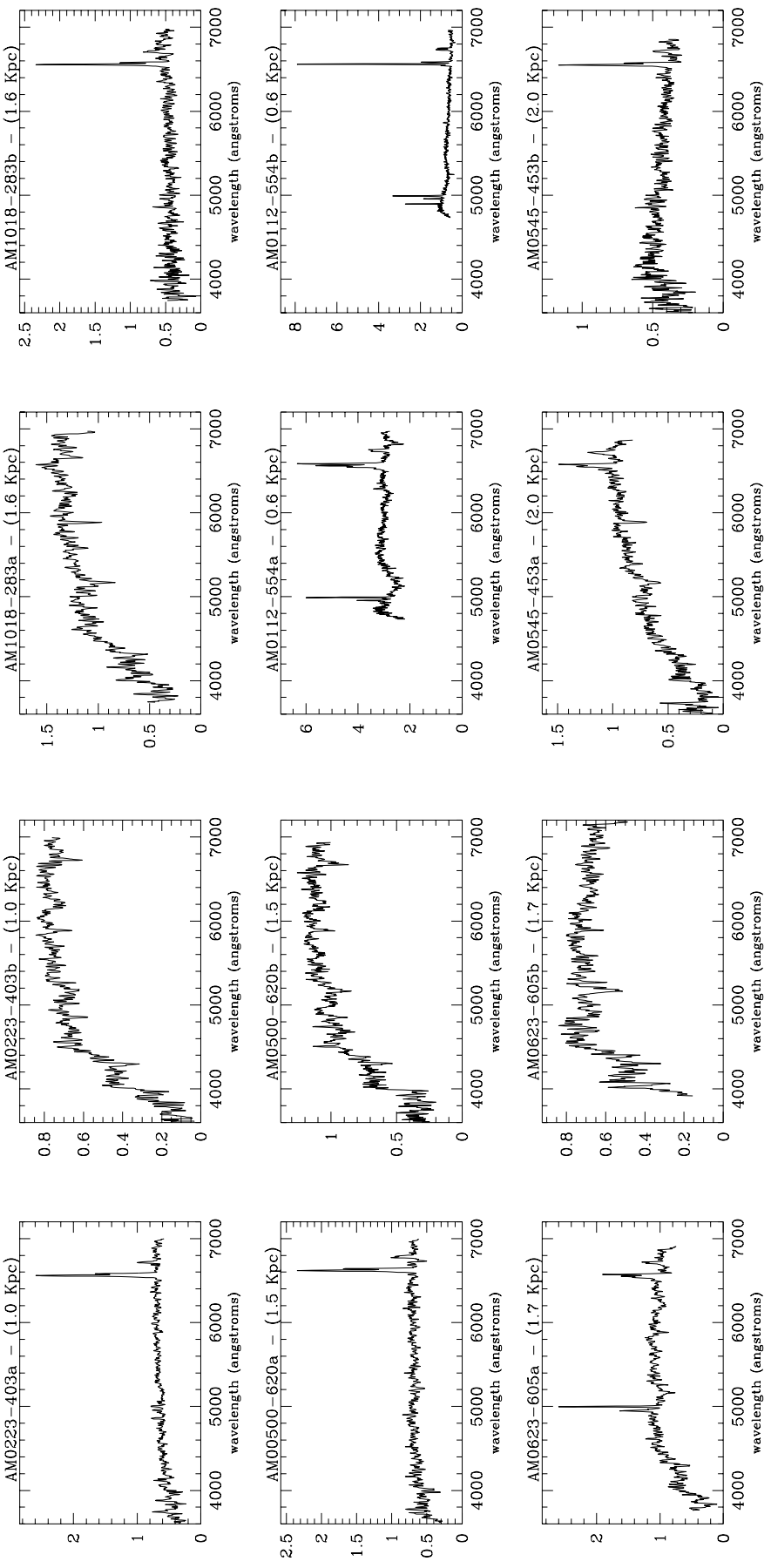

FIG. 2.—*Continued*

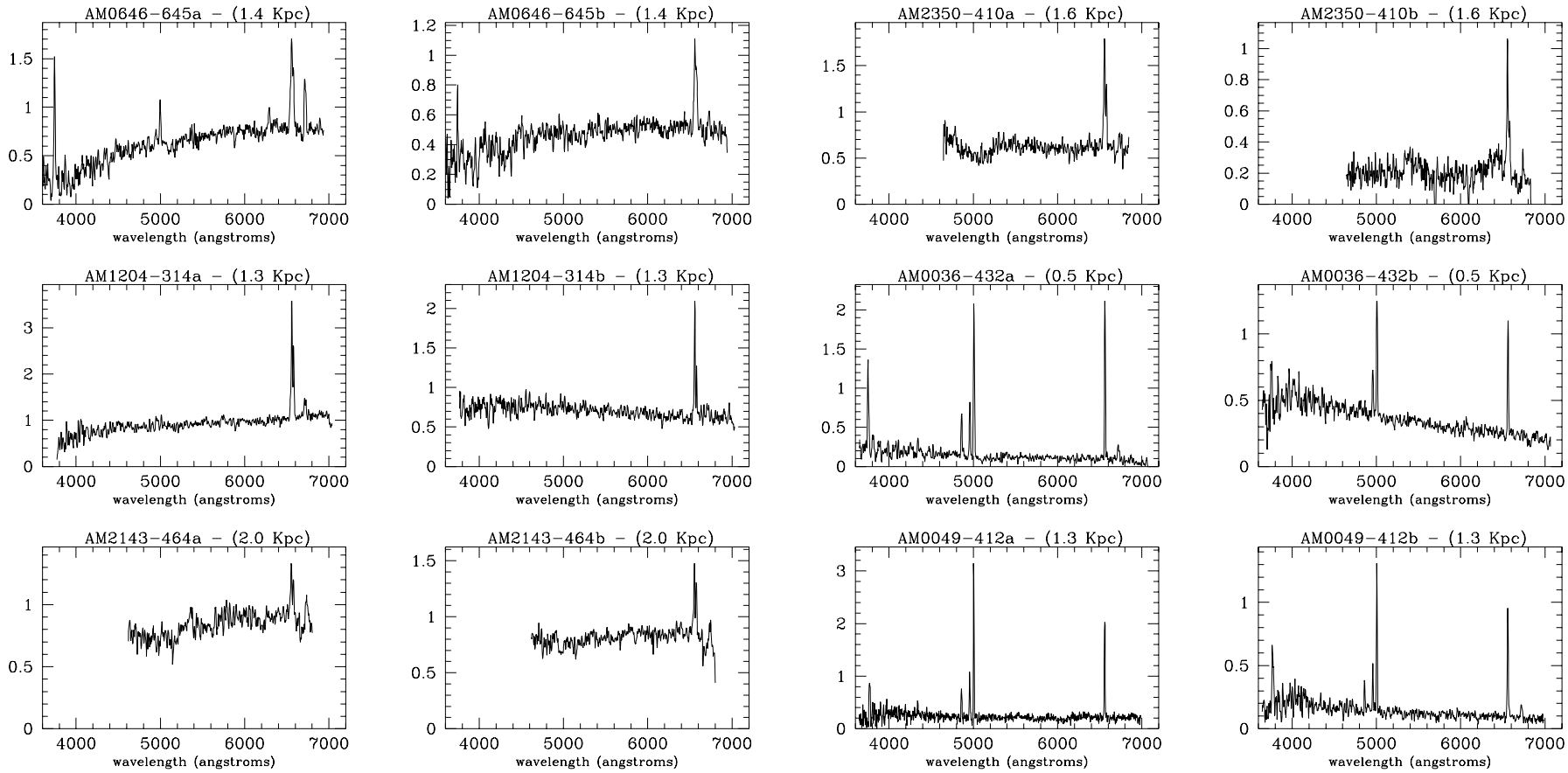

FIG. 2.—*Continued*

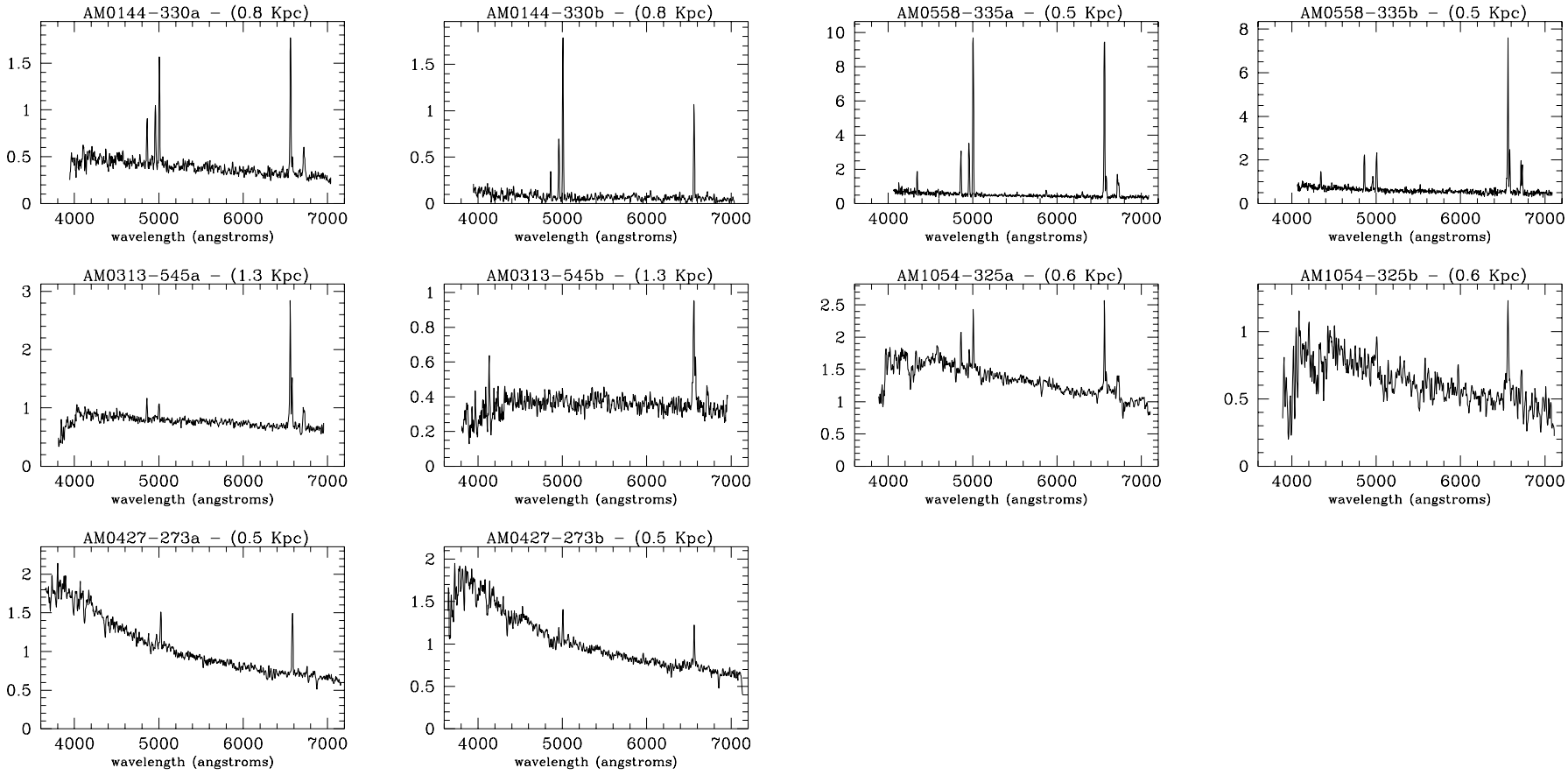

FIG. 2.—*Continued*

TABLE 3

EQUIVALENT WIDTHS AND RADIAL VELOCITIES

	A COMPONENTS			B COMPONENTS		
GALAXY (1)	Hα + [N II] (Å) (2)	[O II] (Å) (3)	cz (km s^{-1}) (4)	Hα + [N II] (Å) (5)	[O II] (Å) (6)	cz (km s^{-1}) (7)
Group 1						
AM 1204−292	...	...	1914	...	...	2241
AM 1325−292	...	...	4431	...	...	4400
AM 2039−241	3	...	5959	...	...	6010
AM 2225−250	...	...	4735	2	...	4358
AM 2244−651	...	...	3362	...	...	3360
AM 2353−291	...	...	8976	4	24	8803
Group 2						
AM 0223−403	48	24	6253	...	...	6366
AM 0500−620	37	...	9005	...	...	8811
AM 0623−605	7	...	12113	...	...	12322
AM 1018−283	...	...	9423	60	...	9188
Group 3						
AM 0112−554	9	...	4251	139	...	4278
AM 0545−453	9	31	12205	38	...	12479
AM 0646−645	22	119	8685	19	19	8410
AM 1204−314	34	...	6765	30	...	7071
AM 2143−464	6	...	11290	10	...	11382
AM 2350−410	34	...	9690	49	...	9919
Group 4						
AM 0036−432	290	103	3245	48	17	3382
AM 0049−412	132	74	7222	140	66	7085
AM 0144−330	71	9	4964	294	...	4982
AM 0313−545	39	...	8442	29	...	8319
AM 0427−545	9	...	868	14	...	920
AM 0558−335	333	...	2925	139	...	2925
AM 1054−325	15	...	3931	31	...	3656
Apparent						
AM 1316−241	4	...	9706	24	...	10330
AM 2252−340	6	...	10038	...	...	8582

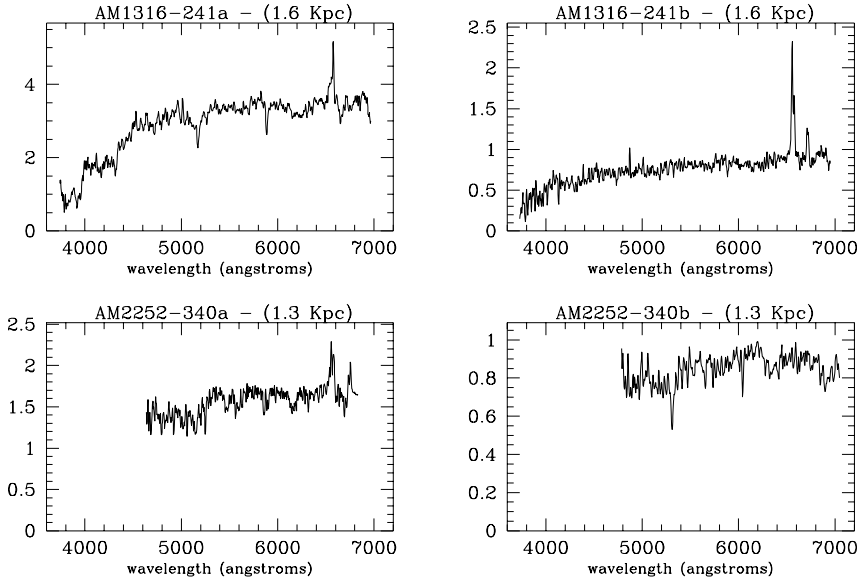

FIG. 3.—Spectra for the apparent mergers

TABLE 4A

FLUX RATIOS (A COMPONENTS)[a]

Galaxy	$E(B-V)$	log ([O II]/Hα)	log ([O III]/Hβ)	log ([O I]/Hα)	log ([N II]/Hα)	log ([S II]/Hα)	Hα
			Group 1				
AM 1204−292.....	...	...	...	...	...	...	...
AM 1325−292.....	...	...	...	...	...	...	...
AM 2039−241.....	...	...	...	...	0.19	−0.06	1.7
AM 2225−250.....	...	...	...	...	...	...	...
AM 2244−651.....	...	...	...	...	...	...	...
AM 2353−291.....	...	...	...	...	...	...	...
			Group 2				
AM 0223−403.....	1.29	0.76	0.08	...	−0.36	−0.78	38.3
AM 0500−620.....	0.83	...	...	−1.15	−0.26	−0.38	25.6
AM 0623−605.....	0.02	...	0.90	−0.40	0.25	0.06	7.0
AM 1018−283.....	...	...	...	...	...	...	...
			Group 3				
AM 0112−554.....	0.24	...	0.61	−0.69	0.20	−0.11	30.4
AM 0545−453.....	...	...	...	...	−0.02	−0.03	8.5
AM 0646−645.....	0.36	0.50	0.36	−0.47	−0.19	−0.07	17.5
AM 1204−314.....	1.62	...	...	...	−0.20	−0.46	35.8
AM 2143−464.....	...	...	...	...	−0.35	0.12	5.7
AM 2350−410.....	...	...	...	...	−0.33	−0.67	21.5
			Group 4				
AM 0036−432.....	0.12	−0.01	0.57	...	−1.36	−0.76	27.9
AM 0049−412.....	0.08	−0.20	0.60	...	−1.41	−1.11	25.0
AM 0144−330.....	0.21	−0.56	0.40	...	−0.98	−0.49	21.9
AM 0313−545.....	0.61	...	−0.08	...	−0.44	−0.47	22.9
AM 0427−545.....	0.18	...	0.40	...	−0.80	−0.80	11.2
AM 0558−335.....	0.30	...	0.58	−1.34	−0.95	−0.64	127.0
AM 1054−325.....	0.06	...	0.29	...	−0.85	−0.24	16.8
			Apparent				
AM 1316−241.....	...	...	...	...	0.17	−0.29	18.9
AM 2252−340.....	...	...	...	...	0.19	0.15	5.7

[a] Hα in units of 10^{-15} ergs cm^{-2} s^{-1}.

produce broad fans of stars when perturbed. These results are listed in Table 5. It is noted that most of the galaxies of groups 1 and 2 are ellipticals and S0, while galaxies of groups 3 and 4 are mostly spirals. Note also that spectroscopic classifications of old populations largely match the morphological classifications of originally elliptical components.

4.3. *Star Formation Rates and Ages of the Star Formation Events*

In this section we analyze the star formation events of the merger galaxies, and we compare them with the results obtained for the interacting pairs described in DP97. As was pointed out by Kennicutt (1983) and Gallagher, Hunter, & Bushouse (1989), the equivalent widths of Hα+[N II] and [O II] λ3727 are very sensitive parameters to measure the relative amount of global star formation in galaxy systems. In order to perform this analysis we have measured the equivalent widths of these emission lines, which are listed in columns (2), (3), (5), and (6) of Table 3. It is observed that the average EW(Hα+[N II]) for the whole sample is 75 Å, higher than the mean value of 50 Å found by Liu & Kennicutt (1995, hereafter L&K95) in a similar sample of merging galaxies, and it is also well above the observed mean value for a sample of interacting pairs, EW(Hα + [N II]) = 37 Å (DP97). Figure 4*a* illustrates this analysis through the distribution function of EW(Hα+[N II]) for the interacting (DP97) and merger samples. Note that equivalent widths larger than 140 Å are only observed in mergers.

Figure 4*b* presents the EW(Hα+[N II]) versus the group number described in the previous section. It is clearly seen that galaxies of groups 2 and 3 have on average EW(Hα+[N II]) = 39 Å, with this value very similar to the observed mean in the DP97 sample and therefore higher than the value of 29 Å reported for normal isolated spiral galaxies (Kennicutt & Kent 1983). On the other hand, group 4 shows a very high mean of the EW(Hα+[N II]) = 113 Å, suggesting a significant enhancement of the SFR when compared to the interacting pairs. This value is even higher than that observed by L&K95 in a subsample of 10 ultraluminous *IRAS* mergers, which show on average EW(Hα+[N II]) = 88 Å.

Many authors (see, for instance, Lequeux et al. 1981; Copetti, Pastoriza, & Dottori 1986; Leitherer & Heckman 1995, hereafter L&H95) have found that certain parameters such as EW(Hα), EW(Hβ), and the ratio [O III]/Hβ decrease monotonically as a function of time and therefore are good star formation age indicators. For our particular case we

TABLE 4B

FLUX RATIOS (B COMPONENTS)[a]

Galaxy	$E(B-V)$	log ([O II]/Hα)	log ([O III]/Hβ)	log ([O I]/Hα)	log ([N II]/Hα)	log ([S II]/Hα)	Hα
			Group 1				
AM 1204−292.....	...	...	...	...	...	...	...
AM 1325−292.....	...	...	...	...	...	...	...
AM 2039−241.....	...	...	...	...	...	...	...
AM 2225−250.....	...	...	...	...	0.69	0.66	0.5
AM 2244−651.....	...	...	...	...	...	...	...
AM 2353−291.....	...	...	...	...	...	...	...
			Group 2				
AM 0223−403.....	...	...	...	...	...	...	...
AM 0500−620.....	...	...	...	...	...	...	...
AM 0623−605.....	...	...	...	...	...	...	...
AM 1018−283.....	0.85	...	−0.17	...	−0.47	−0.49	27.8
			Group 3				
AM 0112−554.....	0.78	...	0.20	...	−0.69	−0.74	76.3
AM 0545−453.....	0.96	...	...	...	−0.48	−0.57	13.6
AM 0646−645.....	...	...	...	...	−0.01	−0.50	14.0
AM 1204−314.....	...	...	...	...	−0.41	−0.52	19.3
AM 2143−464.....	...	...	...	...	−0.20	−0.26	8.4
AM 2350−410.....	...	...	...	...	−0.51	−0.62	11.2
			Group 4				
AM 0036−432.....	0.18	−0.03	0.63	...	−0.91	−0.75	12.7
AM 0049−412.....	0.49	0.40	0.73	...	−1.13	−0.61	13.7
AM 0144−330.....	0.25	...	0.78	...	−1.14	−1.00	14.1
AM 0313−545.....	...	...	...	...	−0.48	−0.39	14.2
AM 0427−545.....	0.69	...	0.54	...	−0.74	−0.75	11.8
AM 0558−335.....	0.17	...	0.03	−1.21	−0.56	−0.45	78.2
AM 1054−325.....	...	...	...	...	−0.81	−0.55	13.3
			Apparent				
AM 1316−241.....	0.72	...	−0.11	...	−0.30	−0.35	23.8
AM 2252−340.....	...	...	...	...	...	...	...

[a] Hα in units of 10^{-15} ergs cm^{-2} s^{-1}.

have adopted the L&H95 models to date the star formation events using the equivalent width of the Balmer lines. These models have been calculated for a population of massive stars using input parameters chosen to correspond to conditions typically found in objects such as H II regions, H II galaxies, blue compact dwarf galaxies, nuclear starburst galaxies, and infrared luminous starburst galaxies.

For galaxies that show both emission and absorption features in their spectra, we choose those models with a constant star formation rate over a time interval of 300 Myr with $\alpha = 2.35$, $M_{up} = 30\ M_{\odot}$, and $Z = 0.5\ Z_{\odot}$. On the other hand, we have assumed the instantaneous star formation models of L&H95 with the same parameters described above for those galaxies that show excited emission region–type spectra. This selection was made since according to the models of Copetti et al. (1986), we observe in these galaxies [O III]/Hβ ratios that are representative of H II regions younger than 10 Myr. Particularly we use the constant star formation rate models on galaxies of groups 2 and 3, while the instantaneous star formation models were used on most galaxies of group 4.

For the star formation events of galaxies that belong to groups 2 and 3, we obtained a mean age of 200 Myr, while for galaxies of group 4, we found a mean value of 7.8 Myr. The mean age values found for groups 2 and 3 are very similar to those obtained to their counterparts in the interacting pairs (DP97). The more recent star-forming events in both samples (mergers and pairs) are found in group 4 of mergers.

4.4. *Diagnostic Diagrams and Nuclear Activity*

Figures 5*a*, 5*b*, and 5*c* plot in a logarithmic scale the classical diagnostic diagrams employed to classify the spectra of extragalactic objects according to the main excitation mechanisms (Veilleux & Osterbrock 1987). The diagrams are [O III] λ5007/Hβ versus [N II] λ6854/Hα, [O III] λ5007/Hβ versus [S II] $\lambda\lambda$6717, 6731/Hα, and [O III] λ5007/Hβ versus [O I] λ6300/Hα. According to these diagrams we find that 6% of the studied spectra are AGNs. Considered separately, Seyfert nuclei are found in two objects (AM 0112−554a and AM 0623−605a) of the sample (4%), and only one object (AM 0646−645a) is a LINER (2%). As a comparison L&K95 report in a similar sample of 28 optically selected mergers no Seyfert nuclei and nine LINERs (16%).

However, according to the same analysis presented in

TABLE 5

MORPHOLOGICAL TYPES

Galaxy	A Component	B Component
	Group 1	
AM 1204−292.....	E	S0
AM 1325−292.....	E	S
AM 2039−241.....	S0	S0
AM 2225−250.....	E	S0
AM 2244−651.....	S	S0
AM 2353−291.....	E	E
	Group 2	
AM 0223−403.....	S0	S
AM 0500−620.....	S	S0
AM 0623−605.....	S	E
AM 1018−283.....	S0	S
	Group 3	
AM 0112−554.....	S0	S
AM 0545−453.....	S	S
AM 0646−645.....	S0	S
AM 1204−314.....	S	S
AM 2143−464.....	S	S
AM 2350−410.....	S	S
	Group 4	
AM 0036−432.....	S	S
AM 0049−412.....	S	S
AM 0144−330.....	E	S
AM 0313−545.....	S	S
AM 0427−545.....	S	S
AM 0558−335.....	S	S
AM 1054−325.....	S	S

PDB99, we note that several objects lie very near the transition zones H II–LINER and H II–Seyfert. Therefore, we used the criteria presented by PDB99 in order to classify those objects that can be described by a combination of a Seyfert + H II region spectra. These galaxies are AM 0049−412b and AM 0558−335a. On the other hand, the galaxies with a spectrum that can be described as a combination of a LINER + H II region spectra are AM 0144−330a, AM 0313−545a, AM 0500−620a, AM 0558−335b, AM 1018−283b, and AM 1054−325a. Note that these galaxies raise the ratio of objects that may host a low−luminosity active nucleus in the sample from 6% to 24%, of which 8% are Syefert galaxies and 14% are LINERs. This fraction is much lower than that found in the interacting sample (DP97) in which almost 40% of the galaxies may have an AGN.

Another interesting point is observed in Figure 5*a*: Merger galaxies present on average much larger values of [O III]λ5007/Hβ than those of the interacting galaxies. We found that this ratio is $\sim$3 for mergers and $\sim$1 for interactings, indicating that merger spectra are of higher excitation than those of the pairs. This fact can be attributed to a lower gas metallicity rather than to the fraction of AGNs involved. The multipurpose code MAPPINGS Ic (Ferruit et al. 1997) was used to compute photoionization models. We found that $Z/Z_{\odot}$ is on average 0.5 for mergers, while $Z/Z_{\odot} = 1$ for interactings (Donzelli & Pastoriza 2000).

5. INFRARED LUMINOSITIES

We have used the 12, 25, 60, and 100 μm *IRAS* fluxes of the galaxies to calculate infrared luminosities and to analyze the nature of the infrared emission for the merger sample and the interacting pairs of DP97.

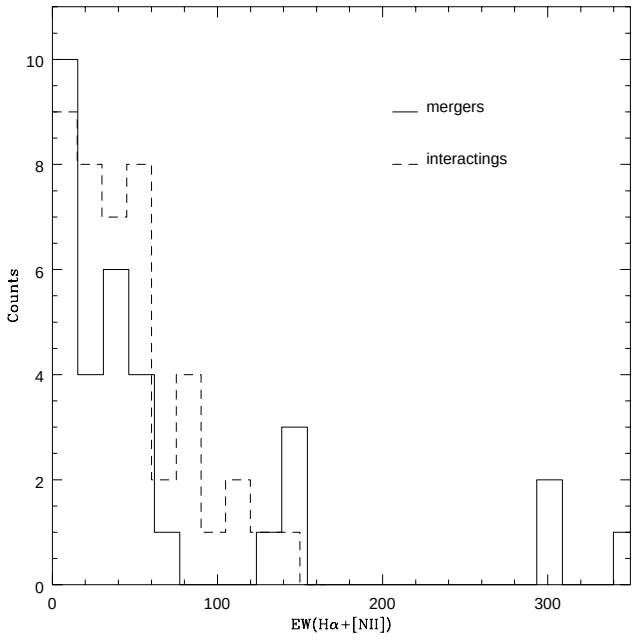

FIG. 4*a*

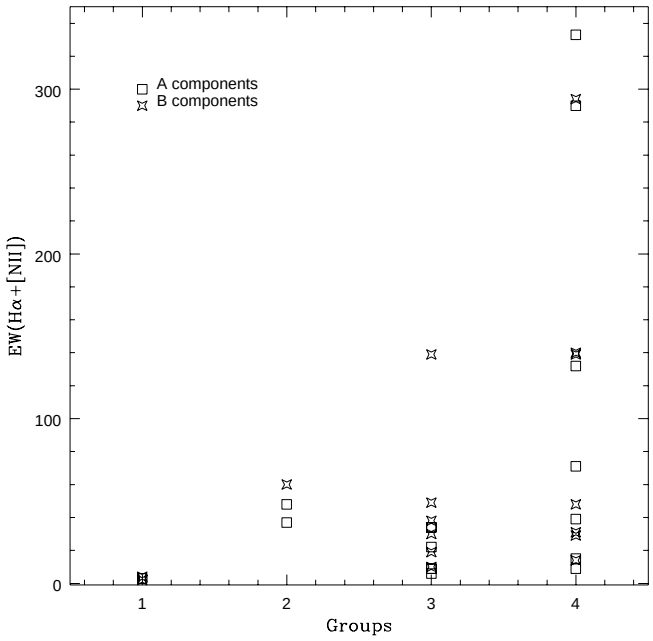

FIG. 4*b*

FIG. 4.—(*a*) EW(Hα + [N II]) distribution function for mergers (*solid line*) and interacting pairs (DP97) (*dashed line*). (*b*) EW(Hα + [N II]) vs. group number as defined in § 4.2 for merger galaxies. Squares represent components A, and stars represent components B.

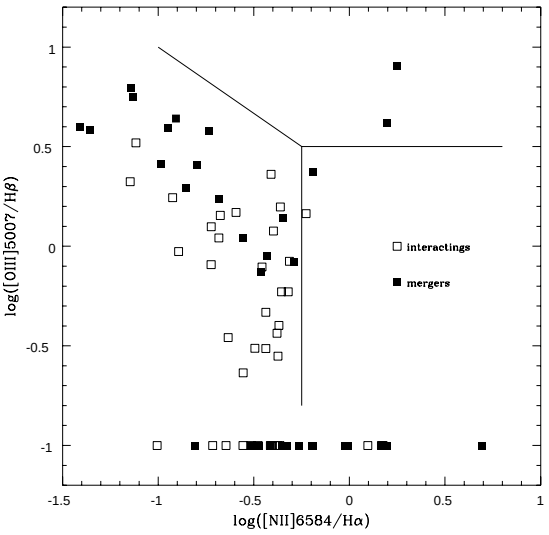

FIG. 5*a*

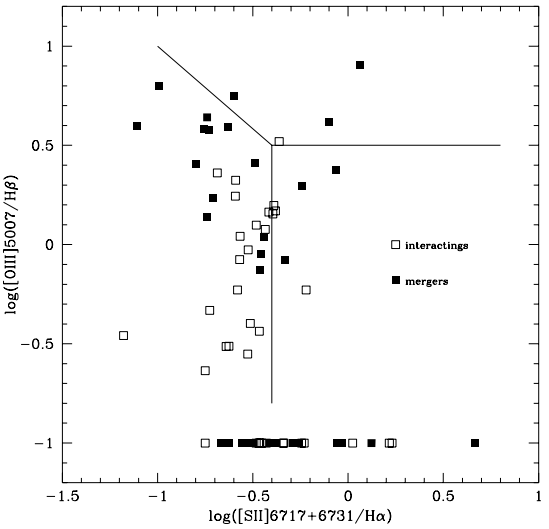

FIG. 5*b*

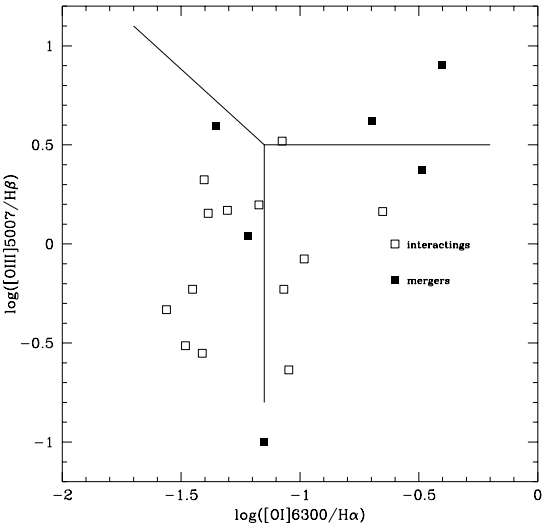

FIG. 5*c*

FIG. 5.—(*a*) [O III] λ5007/Hβ vs. [N II] λ6854/Hα for merger (*open squares*) and interacting pairs (DP97) (*filled squares*). (*b*) Same as (*a*) for [O III] λ5007/Hβ vs. [S II] λλ6717, 6731/Hα ratios. (*c*) Same (*a*) for [O III] λ5007/Hβ vs. [O I] λ6300/Hα ratios.

The luminosities were calculated as follows:

$$F_{\rm ir} = 1.8 \times 10^{-14} \times (13.48 f_{12} + 5.16 f_{25} + 2.58 f_{60} + f_{100})\ [\mathrm{W\ m^{-2}}]$$

$$L_{\rm ir} = 4\pi D_L^2 F_{\rm ir}\ L_\odot\ ,$$

where f_{12}, f_{25}, f_{60}, and f_{100} are the flux densities in janskys at 12, 25, 60, and 100 μm, respectively. D_L^2 is the luminosity distance. According to the infrared luminosity, the galaxies have been classified as follows: luminous infrared galaxies (LIG), $L_{\rm ir} > 10^{11}\ L_\odot$ and ultraluminous infrared galaxies (ULIG), $L_{\rm ir} > 10^{12}\ L_\odot$ (Sanders & Mirabel 1996). *IRAS* fluxes and infrared luminosities in solar units are presented in Table 6.

We are particularly interested in determining if the observed fluxes may result from a combination of dust directly heated by the active galactic nucleus (warm dust), from the host galaxy (cool dust), or a combination of these two processes. For this purpose we have calculated the α(100, 60) and α(25, 12) color indices using the expressions given in Bonatto & Pastoriza (1997, hereafter BP97) and the results are listed in columns (7) and (8) of Tables 6 and 7 for the merger and interacting samples, respectively. These colors are intended to estimate the effect of a cool dust component on Seyfert–pure color indices, taking into account the fact that in normal spiral galaxies the observed 60 and 100 μm fluxes can be almost entirely accounted for by a combination of relatively cool (20–25 K) dust heated by the interstellar radiation field and warmer dust heated by O and B stars (Walterbos & Greenwalt 1996). As a first result, we found that most of the mergers and paired galaxies share the same loci of points than the Seyfert 1 galaxies of BP97, as is shown in Figure 6 which reproduces the α(25, 12) versus α(100, 60) diagram of BP97. This indicates that IR colors of our sample can be explained as a result of dust heated directly by the AGN source with some fraction of emission from cool dust ($0.2 \leq \beta \leq 0.6$) with evaporation

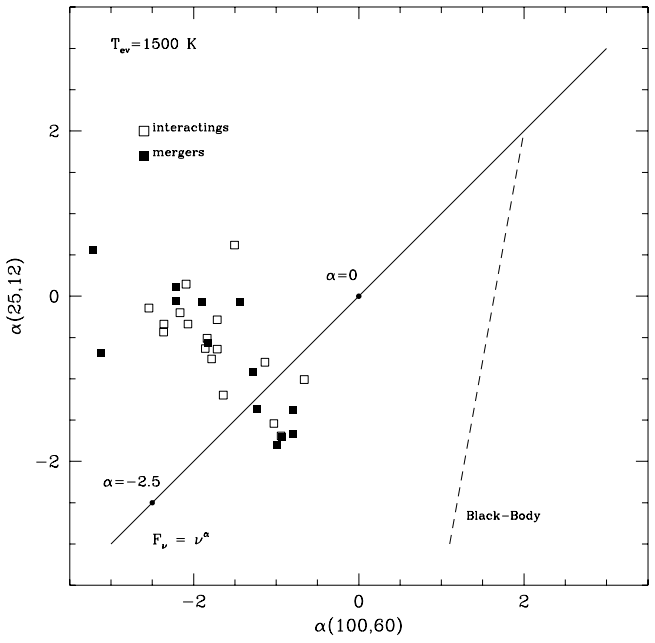

FIG. 6.—Mergers (*filled squares*) and interacting galaxies (DP97) (*open squares*) are plotted on this color-color diagram for dust models with $T_{\rm ev} = 1500$ K.

TABLE 6

IRAS FLUXES, LUMINOSITIES, AND COLORS FOR MERGING GALAXIES

Galaxy (1)	f_{12} (2)	f_{25} (3)	f_{60} (4)	f_{100} (5)	log (L_{ir}) (6)	α(25, 12) (7)	α(100, 60) (8)
			Group 1				
AM 1204−292.....	0.085L	0.141L	0.232	1.123	9.20	−0.69	−3.11
AM 2225−250.....	0.132L	0.137L	0.376	1.157	9.99	−0.05	−2.22
			Group 2				
AM 0223−403.....	0.140	0.381	3.909	7.289	10.93	−1.36	−1.23
AM 0500−620.....	0.057L	0.061	0.413	0.857	10.38	−0.07	−1.44
AM 0623−605.....	0.073L	0.048	0.159	0.814	10.33	0.56	−3.22
			Group 3				
AM 0112−554.....	0.213	0.417	1.476	2.822	11.00	−0.91	−1.28
AM 0545−453.....	0.073	0.110	0.985	2.482	10.81	−0.57	−1.82
AM 0646−645.....	0.092L	0.313	1.459	2.188	11.27	−1.67	−0.80
AM 1204−314.....	0.245	0.679	7.563	10.135	11.09	−1.38	−0.80
			Group 4				
AM 0313−545.....	0.075	0.028	3.440	5.669	8.31	−1.80	−0.99
AM 0427−273.....	0.0612L	0.056L	0.242	0.742L	10.00	0.11	−2.21
AM 0558−335.....	0.102	0.357	1.974	3.168	9.97	−1.70	−0.93
AM 1054−325.....	0.159L	0.168L	0.640	1.675	10.56	−0.07	−1.90

NOTE.—"L" in fluxes stands for upper limit detection. Log of luminosities are expressed in solar units.

temperature of $T_{ev} = 1500$ K. The exceptions are the merger galaxies AM 0223−403, AM 0313−545, AM 0558−335, AM 0646−645, and AM 1204−314 and the interacting pairs AM 2105−332 and AM 1118−350, which are located near the starburst region of the diagram. This result gives additional support to our conclusion that many of these interacting galaxies may host a low-luminosity AGN surrounded by star formation regions. Regarding the total

TABLE 7

IRAS FLUXES, LUMINOSITIES, AND COLORS FOR DP97 GALAXIES

Galaxy (1)	f_{12} (2)	f_{25} (3)	f_{60} (4)	f_{100} (5)	log (L_{ir}) (6)	α(25, 12) (7)	α(100, 60) (8)
			Group 1				
AM 0821−783.....	0.081	0.081L	0.234	1.409	10.07	−0.01	−3.54
AM 2238−575.....	0.092	0.083	0.625	1.812	10.77	0.14	−2.10
			Group 2				
AM 0304−391.....	0.125	0.139	1.159	4.200	10.59	−0.14	−2.54
AM 0728−664.....	0.216	0.250	2.352	7.036	10.66	−0.20	−2.16
AM 0905−232.....	0.128	0.176	1.638	5.406	10.18	−0.43	−2.36
AM 1448−262.....	0.097L	0.233	0.850	1.949	9.66	−1.20	−1.64
AM 2105−332.....	0.091L	0.282L	0.700	1.177	10.26	−1.54	−1.02
			Group 3				
AM 0907−753.....	0.297	0.381	3.425	9.760	10.72	−0.34	−2.07
AM 1127−351.....	0.116	0.143L	0.953	2.268	10.61	−0.28	−1.71
AM 1401−324.....	0.107L	0.156L	0.459	1.165	10.69	−0.51	−1.84
AM 2030−303.....	0.112L	0.180	1.098	2.616	11.09	−0.64	−1.71
AM 2058−381.....	0.061L	0.106L	0.254	0.627	10.62	−0.76	−1.78
			Group 4				
0103−302	0.161	0.256	2.108	5.407	11.12	−0.63	−1.86
AM 1118−350.....	0.073L	0.155	0.570	0.796	11.37	−1.01	−0.66
AM 1219−430.....	0.290	5.237	4.704	8.337	11.38	−3.95	−1.12
AM 1304−333.....	0.155	0.538	4.491	7.240	11.29	−1.69	−0.94
AM 2229−735.....	0.097L	0.062L	0.463	0.992	11.07	0.62	−1.50
AM 2322−821.....	0.192	0.246	2.338	7.732	10.34	−0.34	−2.36

NOTE.—"L" in fluxes stands for upper limit detection. Log of luminosities are expressed in solar units.

infrared luminosity, we have found that on average interacting galaxies present values of log (L_{IR}) greater than merging systems (10.9 and 10.7, respectively). Moreover, in the interacting sample we found that 24% of the pairs are luminous infrared galaxies (LIGs) $L_{ir} > 10^{11}$ $L_{\odot}$ (AM 2030−303, AM 0103−302, AM 1118−350, AM 1219−430, AM 1304−333, and AM 2229−735), while in the merger sample this fraction is only 12% (AM 0112−554, AM 0646−645, and AM 1204−314).

6. CONCLUSIONS

We presented the spectroscopic properties of a sample of 25 pairs of merging galaxies and compared these properties with a similar sample of interacting galaxy pairs. Through a detailed analysis of our observations we conclude the following:

1.Both merging and interacting galaxies show a wide range of spectral types ranging from well-evolved stellar populations (older than 200 Myr) to young stellar systems or H II regions with ages around 8 Myr. However, the more recent star-forming events are found in merger galaxies.

2. Merging galaxies show on average higher excitation spectra than interacting pairs. We found that the mean value for the [O III]/Hβ ratio is $\sim$33 for mergers and $\sim$1 for pairs. This fact could be attributed to a lower gas metallicity.

3. SFRs are much higher (almost a factor of 2) in merging galaxies than in interacting systems, which may indicate that star formation correlates with the strength of the interaction.

4. AGNs comprise at a first glance only 6% of the merger sample. However, this fraction may increase up to 23% if we consider a masking effect of the AGN spectrum by emission from the circumnuclear star-forming regions. The same analysis applied to the interacting DP97 sample shows that this fraction is 38%.

5. The IR colors of most galaxies of our samples can be explained as a result of dust heated directly by a nonthermal (AGN) source, with some fraction of emission from cool dust with evaporation temperature of $T_{ev} = 1500$ K. This result gives additional support to our conclusion that many of these interacting galaxies may host a low-luminosity AGN surrounded by star formation regions.

6. Regarding to the total infrared luminosities we find that merging galaxies show lower log (L_{ir}) than interacting systems (10.7 and 10.9 respectively) and a lower fraction of LIGs (12% vs. 24%).

We acknowledge SECyT, CNPq, ANTORCHAS, VITAE, and PRONEX/FINEP 76.97.1003.00 for financial support. The authors also want to acknowledge the referee for comments and suggestions. Many thanks to Cristian Beauge and John Pritchard for the English revision.

REFERENCES

Arp, H., & Madore, B. F. 1987, A Catalogue of Southern Peculiar Galaxies and Associations (Cambridge: Cambridge Univ. Press) (AMC)
Bica, E. 1988, A&A, 195, 76
Bonatto, C. J., & Pastoriza, M. G. 1997, ApJ, 486, 132 (BP97)
Copetti, M. V. F., Pastoriza, M. G., & Dottori, H. A. 1986, A&A, 156, 111
de Vaucouleurs, G., et al. 1991, The Third Reference Catalogue of Bright Galaxies (New York: Springer) (RC3)
Donzelli, C. J., & Pastoriza, M. G. 1997, ApJS, 111, 181 (DP97)
———. 2000, in preparation
Duc, P.-A., Mirabel, I. F., & Maza, J. 1997, A&AS, 124, 533
Ferruit, P., Binette, L., Sutherland, R. S., & Pécontal, E. 1997, A&A, 32, 73
Gallagher, J. S., Hunter, D. A., & Bushouse, H. 1989, AJ, 97, 700
Heckman, T. M. 1983, ApJ, 268, 628
Ho, L. C., Filippenko, A. V., & Sargent, W. L. W. 1997, ApJ, 487, 568
Hummel, E. 1981, A&A, 96, 111
Joseph, R. D., & Wright, G. S. 1985, MNRAS, 214, 87
Kennicutt, R. C. 1983, ApJ, 272, 54
Kennicutt, R. C., & Keel, W. C. 1984, ApJ, 279, 5
Kennicutt, R. C., & Kent, S. M. 1983, AJ, 88, 1094
Larson, R. B., & Tinsley B. M. 1978, ApJ, 219, 46
Leitherer, C., & Heckman, T. M. 1995, ApJS, 96, 9 (L&H95)
Lequeux, J., Maucherat-Joubert, M., Deharveng, J., & Kunth, D. 1981, A&A, 103, 305
Liu, C. T., & Kennicutt, R. C. 1995, ApJ, 450, 547
Melnick, J., & Mirabel, I. F. 1990, A&A, 231, 19
Osterbrock, D. E. 1989, Astrophysics of Gaseous Nebulae and Active Galactic Nuclei (Mill Valley: University Science Books)
Pastoriza, M. G., Donzelli, C. J., & Bonatto, C. 1999, A&A, 347, 55 (PDB99)
Sanders, D. B., & Mirabel, I. F. 1996, ARA&A, 34, 749
Sanders, D. B., Soifer, B. T., Elias, J. H., Neugebauer, G., & Matthews, K. 1988, ApJ, 328, 35
Stocke, J. T. 1978, AJ, 83, 248
Stone, R. P. S., & Baldwin, J. A. 1983, MNRAS, 204, 347
Tonry, J., & Davis, M. 1979, AJ, 84, 1511
Veilleux, S., & Osterbrock, D. E. 1987, ApJS, 63, 295
Walter bos, R. A. M., & Greenwalt, B. 1996, ApJ, 460, 696